Quantum-mechanical interference in charge exchange between hydrogen and graphene-like surfaces

2012 J. Phys.: Condens. Matter 24 045004

(http://iopscience.iop.org/0953-8984/24/4/045004)

J. Phys.: Condens. Matter **24** (2012) 045004 (9pp) doi:10.1088/0953-8984/24/4/045004

Quantum-mechanical interference in charge exchange between hydrogen and graphene-like surfaces

M Romero[1], A Iglesias-García[1] and E C Goldberg[1,2]

[1] Instituto de Desarrollo Tecnológico para la Industria Química (INTEC-CONICET-UNL), Güemes 3450, CC91, (S3000GLN) Santa Fe, Argentina
[2] Departamento de Ingenieriá de Materiales, Facultad de Ingenieriá Química, UNL, (S3000GLN) Santa Fe, Argentina

E-mail: egold@intec.unl.edu.ar

Received 29 September 2011, in final form 6 December 2011
Published 5 January 2012
Online at stacks.iop.org/JPhysCM/24/045004

Abstract
The neutral to negative charge fluctuation of a hydrogen atom in front of a graphene surface is calculated by using the Anderson model within an infinite intra atomic Coulomb repulsion approximation. We perform an *ab initio* calculation of the Anderson hybridization function that allows investigation of the effect of quantum-mechanical interference related to the Berry phase inherent to the graphene band structure. We find that consideration of the interaction of hydrogen on top of many C atoms leads to a marked asymmetry of the imaginary part of the hybridization function with respect to the Fermi level. Consequently, Fano factors larger than one and strongly dependent on the energy around the Fermi level are predicted. Moreover, the suppression of the hybridization for energies above the Fermi level can explain the unexpected large negative ion formation measured in the scattering of protons by graphite-like surfaces.

(Some figures may appear in colour only in the online journal)

1. Introduction

Many theoretical works based on first-principles density-functional theory are performed in order to provide an atomic level understanding of the interactions between adatoms and graphene. These works discuss mainly the stable configurations of different adatoms such as alkali, hydrogen, or transition metal atoms, on either graphene or graphite [1–8]. Graphene is a two-dimensional sheet of carbon atoms that has singular spectroscopic and transport properties derived from electronic excitations that behave as chiral Dirac quasiparticles. As an open surface, the use of scanning tunnelling microscopy (STM) probes opens the possibility of controlling the positions of adatoms with atomic precision and at the same time switching the magnetic local moments on and off by gating [9–11]. The theoretical analysis of the spectral, thermodynamic, and scattering properties of the adatoms on graphene is performed in most cases by using the Anderson model [12–14]. The single impurity Anderson model provides a suitable framework for describing the lifetime of the impurity levels and the Fano factors arising in local spectroscopy of impurity resonances in graphene. For instance, in the case of a resonant s-wave impurity a strong adsorption site dependence of the Fano factor was found, this anomaly being an example of quantum-mechanical interference related to the phases inherent to the graphene band structure [7]. But important conclusions like this are usually obtained by using very approximate Hamiltonian parameters. The originally developed Hamiltonian for describing magnetic impurities in a metal [15] was naturally extended to treat chemisorption and ion–surface scattering processes [16, 17]. Nowadays, the Anderson Hamiltonian continues to be one of the most used ones for describing experimental results related to charge fractions of ions backscattered by a surface [18–20] and to the electronic transport through single atom contacts [21–24].

The basic and simple idea behind the Anderson model is a mixed basis set of orthonormalized extended solid states $\phi_{\vec{k}}$ and localized atomic states ϕ_a in which the Hamiltonian can be written as the sum of three well differentiated terms, $\hat{H} = \hat{H}_{\text{solid}} + \hat{H}_{\text{atom}} + \hat{H}_{\text{atom-solid}}$. The $\hat{H}_{\text{solid}}$ term corresponds to the diagonalized description of the solid, $\hat{H}_{\text{atom}}$ includes

the one and two electron interactions in the atom site, where only the intra atomic Coulomb repulsion U is involved in the particular case of an s-wave atom. The interaction term $\hat{H}_{\text{atom-solid}}$ concerns the hybridization matrix $V_{\vec{k},a}$ between the solid and atomic states. Anderson in his work presented a useful expression for $V_{\vec{k},a}$ obtained in terms of Wannier functions $\chi_\alpha(\vec{r}-\vec{R}_n)$ belonging to the bands and assuming a Hartree Fock approximation $\hat{H}^{\text{HF}}(\vec{r})$ of the Hamiltonian [15]:

$$V_{\vec{k},a} = \frac{1}{\sqrt{N}} \int \mathrm{d}\vec{r}\, \phi_a^*(\vec{r}) \hat{H}^{\text{HF}}(\vec{r}) \sum_{n,\alpha} \mathrm{e}^{\mathrm{i}\vec{k}\cdot\vec{R}_n} \chi_\alpha(\vec{r}-\vec{R}_n)$$
$$= \frac{1}{\sqrt{N}} \sum_{n,\alpha} \mathrm{e}^{\mathrm{i}\vec{k}\cdot\vec{R}_n} V_{a,\alpha}(\vec{R}_n).$$

It is important to notice that in this expression the orthonormalization condition required for the mixed basis set $\{\phi_{\vec{k}}, \phi_a\}$ is necessarily traduced to an orthonormalized basis set of Wannier functions $\chi_\alpha(\vec{r}-\vec{R}_n)$ and atomic states $\phi_a(\vec{r})$. Thus, the main difficulties are related to *ab initio* calculations of the hopping and on-site energy contributions and this is the reason why in most cases a semiempirical parametrization of the Anderson Hamiltonian terms is used.

In this work we investigate the charge exchange process between a hydrogen atom and a graphene surface. An infinite intra atomic Coulomb repulsion approximation to the Anderson Hamiltonian is used to treat the hydrogen neutral to negative charge fluctuation. This is the most probable charge fluctuation process, taking into account the ionization and affinity energy levels contrasted with the band states of graphene. For an *ab initio* calculation of the Hamiltonian terms we use a bond-pair model Hamiltonian developed previously for systems consisting of interacting atoms [25]. By proposing a mixed basis set involving localized adatom orbitals and extended surface states, and by application of a mean field approximation, the Hamiltonian can be reduced to the form of the single-particle Anderson model [26]. In this way the on-site atom energy and the hybridization term are determined by both the surface band structure and the atomic properties of the one and two electron interactions, including the effects arising from the lack of orthogonality between the adsorbate and substrate orbitals. A very important magnitude is the Anderson hybridization function

$$\Xi_{0\sigma}(\omega) = \sum\nolimits_{\vec{k}} \frac{|V^\sigma_{\vec{k},a}|^2}{\tilde{\omega} - \varepsilon_{\vec{k}}},$$

because from it we can make inferences about many physical properties of interest. For instance, the relation between $\mathrm{Im}\,\Xi_{0\sigma}(\omega)$ and the intra atomic Coulomb repulsion integral (U) determines whether the coupling regime is weak or strong; $\mathrm{Re}\,\Xi_{0\sigma}(\omega)/\mathrm{Im}\,\Xi_{0\sigma}(\omega)$ can be assumed as a prediction of the sensitivity of the Fano factor to local changes in the chemical potential of graphene caused by either doping or gate voltages [27, 7]; $\mathrm{Im}\,\Xi_{0\sigma}(\omega)$ evaluated at the atom energy level ($\omega = \varepsilon_a$) gives the atom level broadening. The resonance structure of the density of states projected on the atom is also intimately related with the hybridization function. All these important quantities allow for an understanding of the adsorption and ion–surface scattering processes. The effect of the quantum-mechanical interference between the neighbouring C atoms is analysed by means of our *ab initio* calculation that allows variation of the number of substrate atoms interacting with the adatom. We will see that the broadening of the affinity level in this system can justify the negative ion fraction measured in the scattering of low energy protons by a highly oriented pyrolytic graphite (HOPG) surface [20].

2. Theory

2.1. Bond-pair model: Anderson Hamiltonian

A model Hamiltonian developed to describe pairs of interacting atoms [26] was generalized to any atom–surface system by assuming that one of the two atoms consists of a system having a quasicontinuum of states (including extended valence and 'localized' or corelike flatband states). A symmetrically orthogonalized [28] mixed basis set of localized adatom orbitals and extended surface states was used in this case to finally reduce the Hamiltonian to the form of the Anderson model:

$$\hat{H} = \sum_{\vec{k},\sigma} \epsilon_{\vec{k},\sigma} \hat{n}_{\vec{k},\sigma} + \sum_\sigma (\epsilon_{\mathrm{I}} + \tfrac{1}{2} U \hat{n}_{a,\bar{\sigma}}) \hat{n}_{a,\sigma}$$
$$+ \sum_{\vec{k},\sigma} (V^\sigma_{\vec{k},a} \hat{c}^\dagger_{\vec{k},\sigma} \hat{c}_{a,\sigma} + \mathrm{h.c}), \qquad (1)$$

where $\vec{k}$ denotes the solid states with energy $\varepsilon_{\vec{k}}$ and a the 'impurity' atom s-valence orbital with energy ε_{I}. Their respective occupation number operators are $\hat{n}_{\vec{k},\sigma} = \hat{c}^\dagger_{\vec{k},\sigma} \hat{c}_{\vec{k},\sigma}$, $\hat{n}_{a,\sigma} = \hat{c}^\dagger_{a,\sigma} \hat{c}_{a,\sigma}$, σ being the spin projection index. The U parameter represents the intra-site electronic Coulomb repulsion in the unique atomic orbital a considered, and $V^\sigma_{\vec{k},a}$ is the hopping integral between the solid and the 'impurity' atom state.

The one electron hybridization term $V^\sigma_{\vec{k},a}$ includes one and two electron contributions determined consistently with a mean field approximation and an overlap expansion of the many body Hamiltonian. Basically the $V^\sigma_{\vec{k},a}$ term is expanded according to the overlap expansion of the orthogonal $\vec{k}$- and a-states:

$$V^\sigma_{\vec{k},a} = V^{\sigma(0)}_{\vec{k},a} - \tfrac{1}{2} S_{\vec{k},a} (V^{\sigma(0)}_{\vec{k},\vec{k}} + V^{\sigma(0)}_{a,a}) + \cdots, \qquad (2)$$

where the superscript (0) indicates that the matrix elements are referred to the states of the isolated subsystems (atom and solid), and $S_{\vec{k},a}$ is the overlap between them. By performing in equation (2) the expansion of the non-perturbed $\vec{k}$-surface states in the atomic states φ_i centred on the different atoms at $\vec{R}_{\mathrm{s}}$ (LCAO),

$$\varphi_{\vec{k},\sigma}(\vec{r}) = \sum_{i,\vec{R}_{\mathrm{s}}} c_i^{\vec{k},\sigma}(\vec{R}_{\mathrm{s}}) \varphi_i(\vec{r} - \vec{R}_{\mathrm{s}}), \qquad (3)$$

and approximating the three-centre integrals consistently with the overlap expansion, it is found that the non-dimeric contributions are cancelled. The hybridization term is finally

recovered as a superposition of the atomic hopping integrals $V_{i,a}^{\sigma\,(\mathrm{dim})}$ defined only with atomic functions orthogonalized in each dimeric subspace $(\vec{R}_a, \vec{R}_s)$ that include the one and two electron interactions within a mean field approximation [26]:

$$V_{\vec{k},a}^{\sigma} = \sum_{i,\vec{R}_s} c_i^{\vec{k},\sigma}(\vec{R}_s) V_{i,a}^{\sigma\,(\mathrm{dim})}(\vec{R}_s, \vec{R}_a). \tag{4}$$

The approximated treatment of the three-centre atomic integrals is crucial in the modelling of the atom–surface complex, since in this form the whole system is rebuilt from the calculation of each elemental dimer. In equation (3) the coefficients $c_\mu^{\vec{k},\sigma}$ correspond to the expansion of $\varphi_{\vec{k},\sigma}(\vec{r})$ in terms of the atomic orbitals φ_μ (now the index μ indicates the site $\vec{R}_s$ and the atomic state i). Now, we want to refer them to the symmetrically orthonormalized atomic basis set $\{\chi_\alpha\}$ assumed in tight-binding-like calculations of the surface electronic structure. Both basis sets are related in the following manner [28]:

$$\chi_\alpha = \sum_\beta (1+S)_{\alpha\beta}^{-1/2} \varphi_\beta, \tag{5}$$

where the elements of the overlap matrix S are defined as $S_{\mu\alpha} = \int \varphi_\mu^* \varphi_\alpha \,\mathrm{d}\tau - \delta_{\mu\alpha}$. From the expansion of $\varphi_{\vec{k},\sigma}(\vec{r})$ in one or other basis set

$$\varphi_{\vec{k},\sigma}(\vec{r}) = \sum_\mu c_\mu^{\vec{k},\sigma} \varphi_\mu = \sum_\alpha \tilde{c}_\alpha^{\vec{k},\sigma} \chi_\alpha \tag{6}$$

and taking into account equation (5), the following relation is obtained between the expansion coefficients:

$$c_\beta^{\vec{k},\sigma} = \sum_\alpha \tilde{c}_\alpha^{\vec{k},\sigma} (1+S)_{\alpha\beta}^{-1/2}. \tag{7}$$

By introducing the expression equation (7) into equation (4), the LCAO expansion of the matrix element $V_{\vec{k},a}^{\sigma}$ is written in terms of quantities referred to the orthonormalized atomic basis set of the substrate:

$$V_{\vec{k},a}^{\sigma} = \sum_\alpha \tilde{c}_\alpha^{\vec{k},\sigma} \tilde{V}_{\alpha,a}^{\sigma\,(\mathrm{dim})}, \tag{8}$$

where $\tilde{V}_{\alpha,a}^{\sigma\,(\mathrm{dim})} = \sum_\lambda (1+S)_{\alpha\lambda}^{-1/2} V_{\lambda,a}^{\sigma}$.

The coefficients $\tilde{c}_\alpha^{\vec{k},\sigma}$ define the density matrix through the following elements:

$$\tilde{\rho}_{\alpha,\beta}^{\sigma}(\varepsilon) = \sum_{\vec{k}} \tilde{c}_\alpha^{\vec{k},\sigma *} \tilde{c}_\beta^{\vec{k},\sigma} \delta(\varepsilon - \varepsilon_{\vec{k}}). \tag{9}$$

An *ab initio* calculation of the non-interacting self energy $\Xi_{0\sigma}(\omega)$ and, therefore, of the hybridization width $\Gamma_\sigma(\omega) = \mathrm{Im}\,\Xi_{0\sigma}(\omega)$ is now possible through the LCAO expansion (8) of $V_{\vec{k},a}^{\sigma}$:

$$\Xi_{0\sigma}(\omega) = \sum_{\alpha,\beta} \tilde{V}_{a,\alpha}^{\sigma\,(\mathrm{dim})} \tilde{V}_{\beta,a}^{\sigma\,(\mathrm{dim})} \int_{-\infty}^{\infty} \mathrm{d}\varepsilon \, \frac{\tilde{\rho}_{\alpha,\beta}^{\sigma}(\varepsilon)}{\omega - \varepsilon - \mathrm{i}\eta}. \tag{10}$$

The one electron energy levels $(\varepsilon_\mathrm{I}, \varepsilon_\mathrm{I} + U)$ of the atom are calculated as the difference between total energies of the atom–surface system without allowing charge transfer (frozen atomic charges) and by taking into account the orthogonalization effects and a mean field approximation of the two electron interactions [26].

2.2. Electronic structure of the graphene surface

In a graphene sheet, the carbon atoms are held together via sp^2-hybridized covalent bonds, while the electronic transport takes place by hopping along the π orbitals which can participate in covalent bonding with adsorbates. In the negative hydrogen formation from the neutral atom the active state corresponds to the affinity level, which resonates mainly with the π-band states.

The electrons in the π-band of graphene can be quite well described using a tight binding (TB) Hamiltonian within the first neighbours approximation [11]. The LCAO expansion of the graphene π-band states in the orthonormalized p_z-atomic states $\chi_{p_z}(\vec{R}_j^{A(B)})$ is

$$\varphi_{\vec{k}}(\vec{r}) = \frac{1}{\sqrt{2N}} \sum_j \Big[\pm \mathrm{e}^{\mathrm{i}\theta(\xi_{\vec{k}})} \mathrm{e}^{-\mathrm{i}\vec{k}\cdot\vec{R}_j^A} \chi_{p_z}(\vec{R}_j^A) + \mathrm{e}^{-\mathrm{i}\vec{k}\cdot\vec{R}_j^B} \chi_{p_z}(\vec{R}_j^B) \Big], \tag{11}$$

where '+' corresponds to the upper (antibonding) band, '−' to the lower (bonding) band and

$$\xi_{\vec{k}} = -t \sum\nolimits_{\vec{\delta}_j (j=1,3)} \mathrm{e}^{-\mathrm{i}\vec{k}\cdot\vec{\delta}_j},$$

where $\theta(\xi_{\vec{k}}) = \arg(\xi_{\vec{k}})$ and

$$\vec{\delta}_1 = \frac{a}{2}(1, \sqrt{3}), \qquad \vec{\delta}_2 = \frac{a}{2}(1, -\sqrt{3})$$
$$\text{and} \qquad \vec{\delta}_3 = -a(1, 0).$$

The lattice parameter a is 1.42 Å and the hopping t is assumed equal to 2.7 eV.

In figure 1 we show diagonal and crossed in site elements of the density matrix (equation (9)) calculated within the TB approximation, for the π-band of graphene.

2.3. Infinite U approximation of the Anderson Hamiltonian

The most relevant charge fluctuation process is between H^0 and H^-; if it is accomplished $\varepsilon_\mathrm{I} \ll \varepsilon_\mathrm{F}$, $\varepsilon_\mathrm{I} + U > \varepsilon_\mathrm{F}$ and $\Gamma/U < 1$, where ε_F is the Fermi level of the surface and Γ is the hybridization width. In this case the change from the one electron configurations $|\uparrow, 0\rangle, |0, \downarrow\rangle$ to the two electron configuration $|\uparrow, \downarrow\rangle$ involves a spin fluctuation that is treated by assuming holes instead of electrons. The following notation is used:

$$|\uparrow, \downarrow\rangle \Rightarrow |0\rangle \text{ for zero holes.}$$
$$|\uparrow, 0\rangle; |0, \downarrow\rangle \Rightarrow |\sigma\rangle \text{ for one hole with 'spin } \sigma\text{'.}$$

Taking into account this notation, the Hamiltonian that describes the 'impurity' atom can be written as

$$H_\mathrm{at} = E_0 |0\rangle\langle 0| + E_1 (|\uparrow\rangle\langle\uparrow| + |\downarrow\rangle\langle\downarrow|). \tag{12}$$

In equation (12) we have considered spin degeneration, and the total energies E_i are related to the ε_I and U parameters

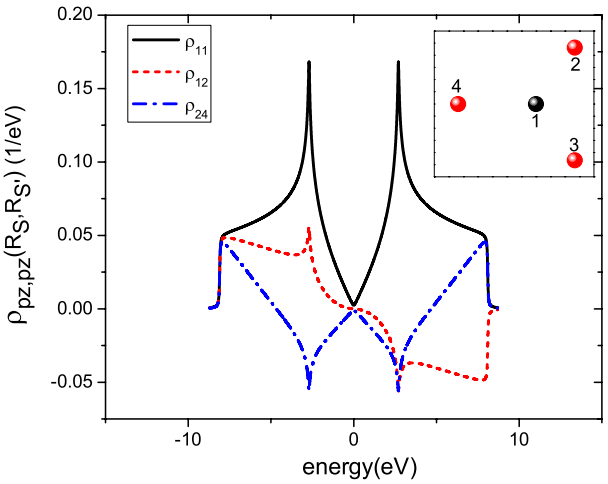

Figure 1. Diagonal and off-diagonal elements of the density matrix for the graphene π-band calculated within the tight binding approximation. The site notation corresponds to the atom sites indicated in the inset.

of equation (1), defining the affinity level in the following way:

$$E_0 - E_1 = (\varepsilon_I + U).$$

The correct normalization of the subspace including the selected atomic configurations is

$$|0\rangle\langle 0| + |\uparrow\rangle\langle\uparrow| + |\downarrow\rangle\langle\downarrow| = \hat{1}. \tag{13}$$

We also have to write down the interaction Hamiltonian within the spirit of the Anderson model which involves only one electron atom–solid interaction terms. The transitions between one and two electrons in the atom can be written as

$$\sum_{\vec{k}} V^{\uparrow}_{\vec{k},a}\hat{c}^{\dagger}_{\vec{k},\uparrow}\hat{c}_{a,\uparrow} \equiv \sum_{\vec{k}} V^{\uparrow}_{\vec{k},a}\hat{c}^{\dagger}_{\vec{k},\uparrow}|0,\downarrow\rangle\langle\uparrow,\downarrow|,$$
$$\sum_{\vec{k}} V^{\downarrow}_{\vec{k},a}\hat{c}^{\dagger}_{\vec{k},\downarrow}\hat{c}_{a,\downarrow} \equiv -\sum_{\vec{k}} V^{\downarrow}_{\vec{k},a}\hat{c}^{\dagger}_{\vec{k},\downarrow}|\uparrow,0\rangle\langle\uparrow,\downarrow|.$$

These terms written within the picture of holes are given by the expression

$$\sum_{\vec{k},\sigma}(-1)^{p_\sigma}\, V^{\sigma}_{\vec{k},a}\hat{c}^{\dagger}_{\vec{k},\sigma}|\sigma\rangle\langle 0|,$$

$$\text{where } p_\sigma = \begin{cases} 0 & \text{si } \sigma = \uparrow, \\ 1 & \text{si } \sigma = \downarrow . \end{cases}$$

Finally, the Anderson Hamiltonian (equation (1)) when only spin fluctuations in the $H^0 \leftrightarrow H^-$ transition are considered is

$$\hat{H} = \sum_{\vec{k},\sigma}\varepsilon_{\vec{k}}\hat{n}_{\vec{k},\sigma} + E_0|0\rangle\langle 0| + E_1\sum_{\sigma}|\sigma\rangle\langle\sigma|$$
$$+ \sum_{\vec{k},\sigma}(-1)^{p_\sigma}\left[V^{\sigma}_{\vec{k},a}\hat{c}^{\dagger}_{\vec{k},\sigma}|\sigma\rangle\langle 0| + V^{\sigma *}_{\vec{k},a}|0\rangle\langle\sigma|\hat{c}_{\vec{k},\sigma}\right]. \tag{14}$$

Equation (14) defines our basic Hamiltonian. We can calculate the probabilities of the selected atomic configurations by means of the following advanced Green function in the static case and for equilibrium processes:

$$G^{\sigma}(t,t') = \mathrm{i}\theta(t'-t)\langle\{|0\rangle\langle\sigma|_{t'}, |\sigma\rangle\langle 0|_t\}\rangle, \tag{15}$$

while for time-dependent or non-equilibrium stationary processes we require also to calculate the following Green–Keldysh functions [29, 30]:

$$F^{\sigma}(t,t') = \mathrm{i}\langle[|0\rangle\langle\sigma|_{t'}, |\sigma\rangle\langle 0|_t]\rangle. \tag{16}$$

The [ ] and { } symbols indicate commutator and anticommutator respectively; and ⟨ ⟩ means the average over the Heisenberg state Φ_0 that describes the interacting system. The probabilities of atomic configurations having one electron (one hole) (n_σ) or two electrons (zero holes) (n_2) are calculated from the corresponding spectral density $\rho^{\sigma}(\omega) = \frac{1}{\pi}\,\mathrm{Im}\,G^{\sigma}(\omega)$ as

$$n_2 = \langle|0\rangle\langle 0|\rangle = \int_{-\infty}^{\infty} \mathrm{d}\omega f_{\prec}(\omega)\rho^{\sigma}(\omega),$$
$$n_\sigma = \langle|\sigma\rangle\langle\sigma|\rangle = \int_{-\infty}^{\infty} \mathrm{d}\omega\,(1 - f_{\prec}(\omega))\rho^{\sigma}(\omega),$$

where $f_{\prec}(\omega)$ is the Fermi function. The following normalization property is valid:

$$\int_{-\infty}^{\infty}\mathrm{d}\omega\,\rho^{\sigma}(\omega) = \langle|0\rangle\langle 0|\rangle + \langle|\sigma\rangle\langle\sigma|\rangle.$$

The Green function given by equation (15) is calculated using the EOM method closed up to a strict order $(V^{\sigma}_{\vec{k},a})^2$ which leads to the following expression [31] ($\tilde{\omega} = \omega - \mathrm{i}\eta$):

$$G^{\sigma}(\omega) = \frac{1 - n_{\tilde{\sigma}} - I_{\tilde{\sigma}}(\omega)}{\tilde{\omega} - \varepsilon_I - U - \Xi_{0\sigma}(\omega) - \Xi_{\prec\tilde{\sigma}}(\omega)}. \tag{17}$$

The quantities $I_{\tilde{\sigma}}(\omega)$ and $\Xi_{\prec\tilde{\sigma}}(\omega)$ introduced in equation (17) are

$$I_{\sigma}(\omega) = \sum_{\vec{k}} V^{\sigma *}_{\vec{k},a}\frac{\langle|0\rangle\langle\sigma|c_{\vec{k},\sigma}\rangle}{\tilde{\omega} - \varepsilon_{\vec{k}}},$$
$$\Xi_{\prec\sigma}(\omega) = \sum_{\vec{k}}\frac{|V^{\sigma}_{\vec{k},a}|^2}{\tilde{\omega} - \varepsilon_{\vec{k}}}\langle 1 - \hat{n}_{\vec{k},\sigma}\rangle,$$

where

$$\langle|0\rangle\langle\sigma|c_{\vec{k},\sigma}\rangle = \frac{\mathrm{Im}}{\pi}\int_{-\infty}^{\infty}\mathrm{d}\omega f_{\prec\sigma}(\omega)\frac{V^{\sigma}_{\vec{k},a}}{\tilde{\omega} - \varepsilon_{\vec{k}}}G^{\sigma}(\omega)$$

and $\Xi_{0\sigma}(\omega)$ is the non-interacting self-energy given by equation (10). Similar expressions to equation (10) are obtained for $I_{\sigma}(\omega)$ and $\Xi_{\prec\sigma}(\omega)$ by using equations (8) and (9).

3. Results and discussion

3.1. Hybridization function

The atomic hopping integral $V^{\sigma(\mathrm{dim})}_{i,a}$ between the 1s state of H and the $2p_z$ state of C is shown in figure 2. In this figure the hopping integral is shown as a function of H distance to the different neighbouring carbon atoms. The H atom is placed

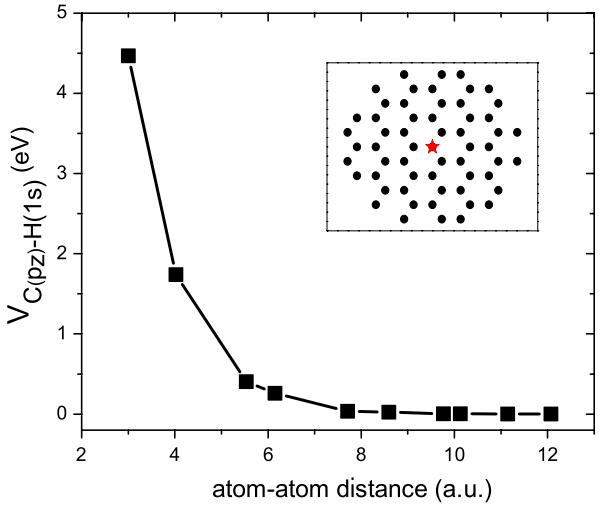

Figure 2. The atomic hopping integral between C $2p_z$ and H 1s states as a function of distance to the different C neighbouring shells shown in the inset. The hydrogen position is on top at 3 au from the surface (star in the inset).

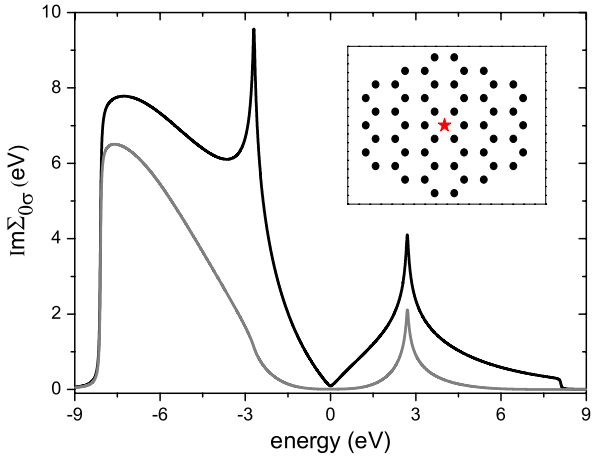

Figure 3. Hybridization functions for H interacting with the graphene π-band at the on top position (black solid line) and at the centre of the hexagon (grey solid line). The hydrogen atom is placed at 3 au from the surface. The on hollow position is shown by a star symbol in the inset.

at 3 au from the surface on top of the central C atom, as is shown in the inset of figure 2. The atomic basis sets used in this calculation are taken from [32].

In figure 3 we compare the hybridization functions, Im $\Xi_{0\sigma}(\varepsilon)$, for the on top and on hollow positions and including all the C neighbours that are able to interact with the adatom at 3 au from the surface. In the on top position there are 58 carbon atoms involved while in the on hollow position there are 54 (see the insets of figures 2 and 3). The orthonormalized hopping matrix in equation (10) is calculated by taking into account the overlap matrix defined in the corresponding subspace with the same number of C atoms.

From figure 3 we can see that the adatom at the hollow site has an essentially flat and zero hybridization with the graphene sheet near the Fermi energy, while in the case of the on top position the hybridization function vanishes linearly near the Fermi energy, reflecting the linear DOS of the graphene. Interestingly, the hybridization functions are very different for energies below and above the Fermi level. In both adsorption positions the hybridization is more important for negative energies. We can say that the interference between C neighbouring atoms interacting with hydrogen has a constructive effect in the bonding valence band while it is destructive in the case of the antibonding upper band.

It is also observed from figure 3 that, in contrast to what happens in the Li case [33], for the hydrogen atom the hybridization function is strongly dependent on the adsorption site. This fact is due to the less extended behaviour of the atomic hydrogen state, as can be seen from figure 2. There is a more significant hybridization in the on top position which is found to be the most stable adsorption site [34, 35, 4].

The importance of considering the interference effects can be seen in figure 4. In figure 4(a) a comparison is made of the hybridization functions calculated in the case of H on top at 3 au from the surface by including only the interaction with the C atom below, with the first four, with 19 and with 58 neighbouring carbon atoms. In this figure we can see that consideration of 19 neighbours is quite enough. The other way, with the on top adatom interacting with only one substrate atom, does not provide a correct description. It is necessary to include at least the first neighbours to take into account the marked asymmetry in the energy dependence of the hybridization function around the Fermi level and the very different behaviour above and below the Fermi level. Figure 4(b) corresponds to the H placed above the middle of the hexagon in which case the hydrogen atom interacts with at least six C atoms. It is observed in this case that the interaction with the first neighbours is good enough to describe satisfactorily the energy dependence of the hybridization function.

The energy dependence of the hybridization function can be understood from the $\vec{k}$ dependence of the coupling term $|V^{\sigma}_{\vec{k},a}|^2$ shown in figures 5(a) and (b) for on top and on hollow adsorption sites respectively.

For $\vec{k}$ values near the $\Gamma(\vec{k}=0)$ point $|V^{\sigma}_{\vec{k},a}|^2$ reaches its maximum value in the bonding band while in the antibonding band it is minimum in the on top case and zero in the hollow site. The corresponding values are determined by the way in which the atomic hopping decays with distance (figure 2). We observe practically no dependence with $\vec{k}$ around the Γ point when all the effective interacting C atoms are included. By comparing in the on top case the $|V^{\sigma}_{\vec{k},a}|^2$ calculated by including the interaction with only one or many C atoms, we can see that the interference between the C atoms has a constructive effect in the bonding band and a destructive character in the antibonding band. The peak structure for energies around ± 2.7 eV ($\vec{k}=M=\frac{2\pi}{3a}(1,0)$) is maintained, but it is strongly diminished for the upper band energies in which the interference terms have a strong destructive effect on $|V^{\sigma}_{\vec{k},a}|^2$. The important differences in the on hollow position (figure 5(b)) are the disappearance of the peak structure at -2.7 eV ($\vec{k}=M$) and the negligible values of $|V^{\sigma}_{\vec{k},a}|^2$ near the Fermi level ($\vec{k}=K=\frac{2\pi}{3a}(1,\frac{1}{\sqrt{3}})$). All these results are

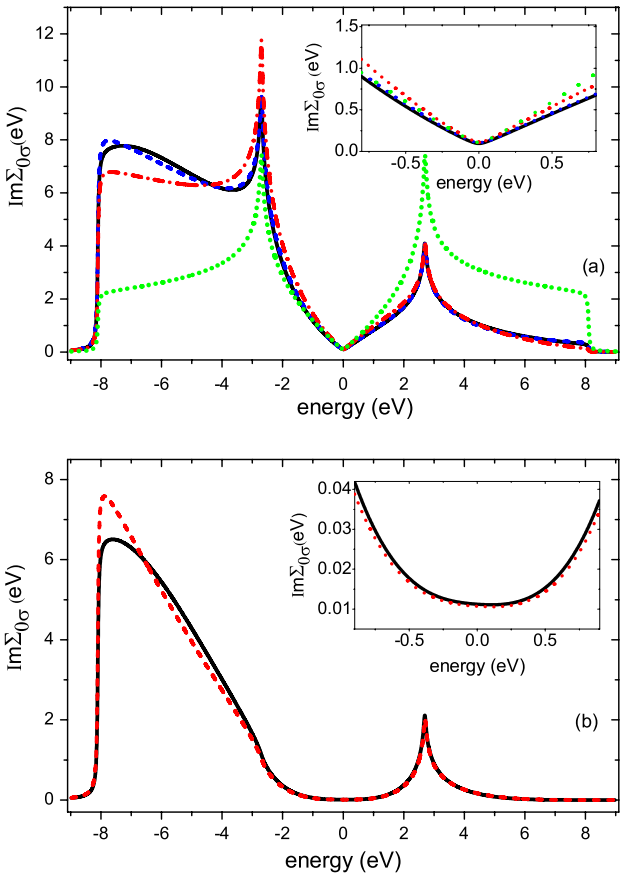

Figure 4. The energy dependence of the hybridization width Im $\Xi_{0\sigma}$. (a) In the case of hydrogen on top at 3 au from the graphene, by considering the interaction with 58 carbon atoms (solid line), with 19 (dashed line), with 4 (dashed–dotted line) and with only one carbon atom (dotted line) (see the inset of figure 2). (b) In the case of hydrogen above the middle of the hexagon at 3 au from the surface, by considering the interaction with 54 carbon atoms (solid line) and with the first six neighbours (dash line) (see inset of figure 3). The insets are a blow up to show the details around the Fermi level.

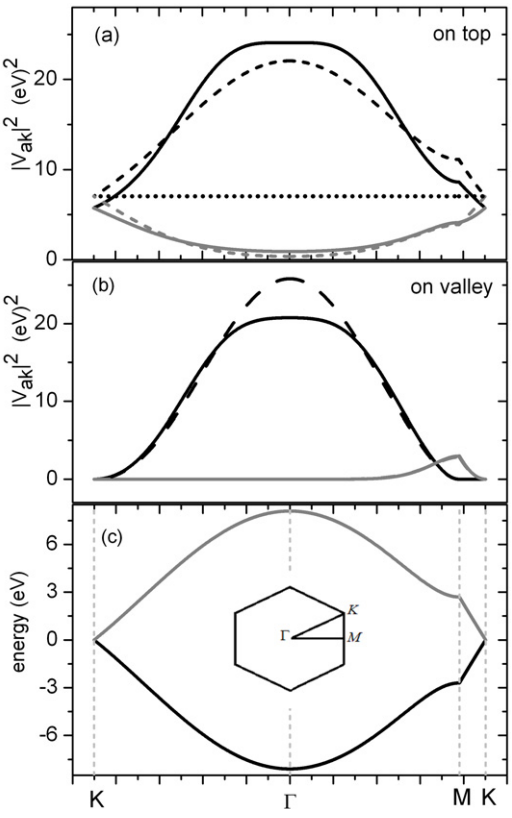

Figure 5. (a) The square modulus $|V^{\sigma}_{\vec{k},a}|^2$ as a function of $|\vec{k}|$ for the H on top at $z = 3$ au. The black lines correspond to the valence band, and the grey lines to the conduction band: calculation including all the C atoms that are capable of interacting (solid lines); the one including the four nearest neighbours (dashed line); and the calculation including only the C below the H atom (dotted line). (b) The same as (a) for hydrogen placed at the centre of the hexagon: calculation including all the C atoms that are capable of interacting (solid lines); and the one including the six nearest neighbours (dashed line). (c) The band energies $\varepsilon_{\vec{k}} = \pm\sqrt{\xi^*_{\vec{k}}\xi_{\vec{k}}}$ as a function of $|\vec{k}|$.

striking examples of quantum-mechanical interference related to the Berry phase, $\theta(\xi_{\vec{k}}) = \arg(\xi_{\vec{k}})$, inherent to the graphene band structure [11]. This can be seen by analysing the LCAO expansion of $V^{\sigma}_{\vec{k},a}$ and taking into account that $|\xi_{\vec{k}}| = 0$ for $\vec{k} = K$, $\theta(\xi_{\vec{k}}) = 2\pi/3$ for $\vec{k} = M$ and $\theta(\xi_{\vec{k}}) = \pi$ for $\vec{k} = \Gamma$. For instance, in the on top position and considering the first four neighbours, we have the following expression:

$$V^{\sigma}_{\vec{k},a} = \frac{1}{\sqrt{2N}}\left[\pm e^{i\theta(\xi_{\vec{k}})}\tilde{V}_{a,C}(\vec{R}) + \tilde{V}_{a,C}(\vec{R} - \vec{\delta}_1)\frac{|\xi_{\vec{k}}|}{-t}e^{-i\theta(\xi_{\vec{k}})}\right],$$

while in the on hollow position and considering the first six neighbours

$$V^{\sigma}_{\vec{k},a} = \frac{1}{\sqrt{2N}}\tilde{V}_{a,C}(\vec{R} - \vec{\delta}_1)\frac{|\xi_{\vec{k}}|}{-t}\{\pm e^{2i\theta(\xi_{\vec{k}})} + e^{-i\theta(\xi_{\vec{k}})}\}.$$

3.2. Energy levels and widths

The analysis of the atom energy levels as a function of atom–surface distance (z) allows one to make inferences about the possibility of resonant charge transfer processes. The ionization and affinity levels of the hydrogen atom calculated by using the bond-pair model [26] are shown in figure 6 contrasted with the graphene π- and σ-band states. The shift by the image potential at large distances is accounted for and the short range interactions are properly considered within the mean field approximation. The pronounced down shift at distances close to the surface ($z = 0$) is mainly due to the attractive interaction with the nuclei. Figure 6 shows from a purely energetic point of view that the fluctuation between neutral and negative charge is the most probable.

The affinity level and $\Gamma_A = 2\,\mathrm{Im}\,\Xi_{0\sigma}(\varepsilon_I(z) + U(z))$ are shown in figure 7. The quantity Γ_A gives an estimation of the widening of the energy level by the interaction, but it only represents correctly the level width in the case of a flat band. The results in figure 7 correspond to the on top site, by considering all the C atoms that effectively interact in figure 7(a), the four nearest neighbours in figure 7(b) and only the C atom below in figure 7(c). The energy level variation with the distance to the surface, calculated by using

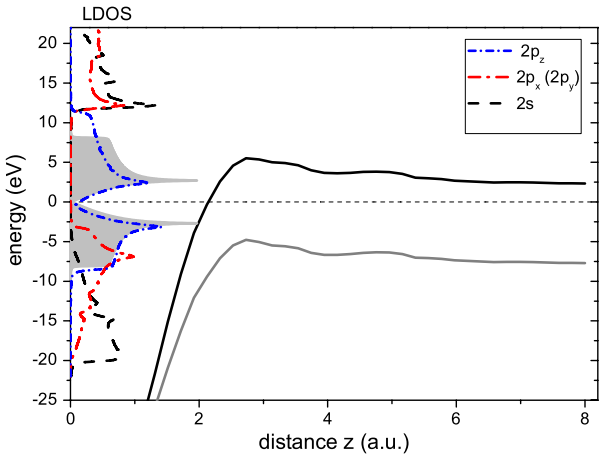

Figure 6. Energy levels of a H atom placed on top of a carbon atom as a function of the distance to the surface. The black (grey) line is the affinity (ionization) level. The shadowed region is the LDOS of the π-band calculated in this work. The s and p LDOS of graphene calculated using the fireball method of [36] are also shown. The energies are referred to the Fermi energy set equal to 0.

the bond-pair model [26], is consistent with the number of C atoms in each case. An upward shift of the affinity level is found for distances between 4 and 2.5 au due to the interaction with many C atoms (figure 7(a)).

The most striking feature of figure 7 is the diminution of Γ_A for energies above the Fermi level caused by the interference effects. The weak coupling regime, characterized by a relation $\Gamma/U < 1$ that validates the infinite U-limit approximation, is achieved for distances $\geq$2 au only in the case of including the interaction with more than one C atom (see also figure 6).

3.3. Adatom local density of states and double occupation

The density of states projected on the atom state (LDOS) is shown in figure 8(a) for the case of hydrogen on top and distant 2.4 au from the surface. In this figure the LDOS is compared for the cases of hydrogen interacting with one, four and all the C atoms that it can see. The resonance structure depends strongly on both the hybridization function and the atom level position. According to equation (17) the energy resonance positions are the solutions of $\omega - \varepsilon_{\rm I} - U = {\rm Re}[\Xi_{0\sigma}(\omega) + \Xi_{<\sigma}(\omega)]$, which can be seen in the inset of figure 8(a). The inclusion of many C atoms in the interaction moves the atom level resonance to energies above the Fermi level, giving in this form a double occupation notably smaller than in the case of considering the interaction with only the first neighbour. The double occupation probability $n_2 = \langle|\uparrow\downarrow\rangle\langle\uparrow\downarrow|\rangle$ is shown as a function of distance to the surface in figure 8(b). The interferences associated with the crossed terms of the density matrix lead to a smaller probability of double occupation for distances close to the surface, while consideration of the interaction with only one surface atom underestimates the negative charge probability for large distances ($z > 3.5$ au).

In figure 9(a) one can see that Re $\Xi_{0\sigma}(\omega)$ is antisymmetric with respect to the Fermi energy in the case of considering

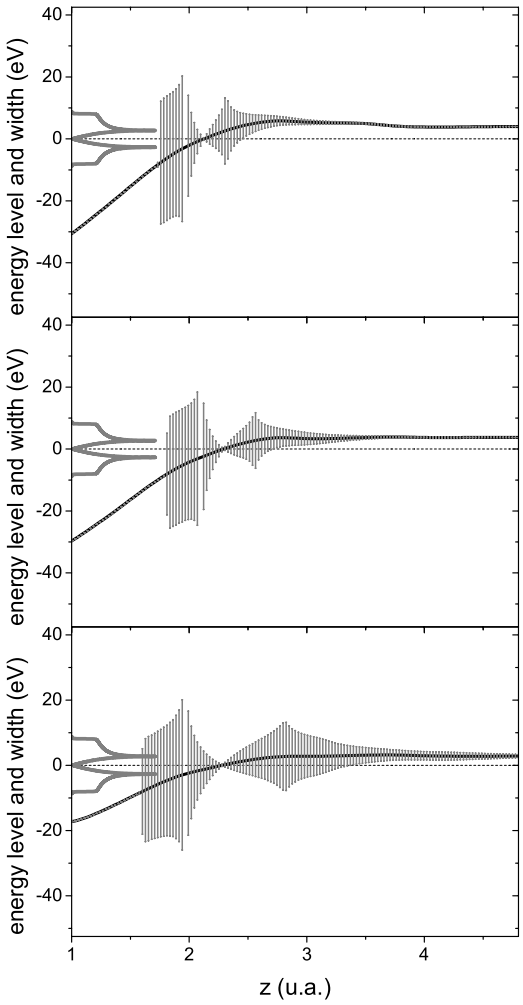

Figure 7. The hydrogen level and Γ_A (shown as error bars) as a function of distance for the on top position, by considering (a) all the effective interacting C atoms, (b) the first four neighbours and (c) only the C atom below.

the interaction with only one C atom. This fact is due to the symmetry of the π-band density of states calculated within the first neighbour tight binding approximation. The marked loss of symmetry of Im $\Xi_{0\sigma}(\omega)$ caused by the quantum interference between the neighbouring C atoms leads to an Re $\Xi_{0\sigma}(\omega)$ different from zero at the Fermi level. The relation between Re $\Xi_{0\sigma}(\omega)$ and Im $\Xi_{0\sigma}(\omega)$ can be viewed as an *ab initio* prediction of the Fano q factor [7]. We find that $q = {\rm Re}\,\Xi_{0\sigma}(\omega)/{\rm Im}\,\Xi_{0\sigma}(\omega)$ is strongly energy-dependent and larger than 1 around the Fermi level in the case of considering the interaction not only with the carbon below the hydrogen atom but also with the first neighbours (figure 9(b)). Therefore, a Fano factor sensitive to local changes in the chemical potential of graphene caused by either doping or gate voltages can be expected.

3.4. Negative ion fraction

In a collision process the negative charge state becomes probable when the hydrogen atom is close to the surface due to the downshift and width of the affinity level. The possibility of

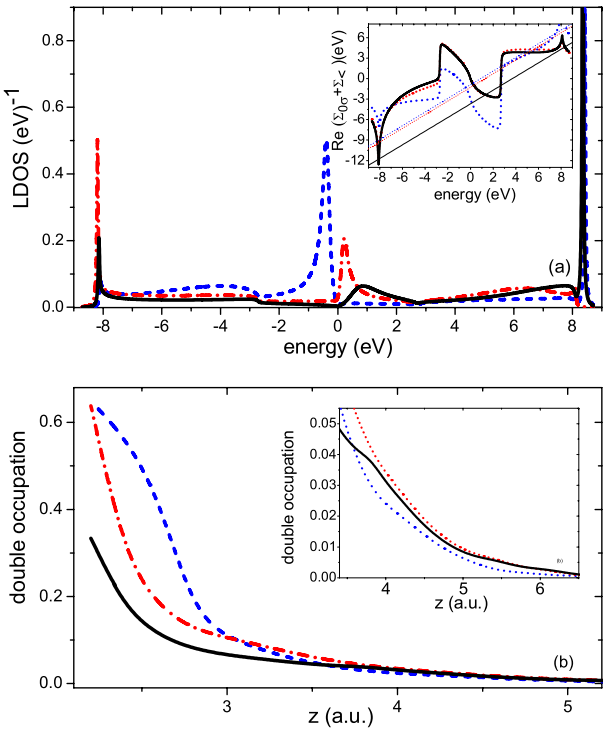

Figure 8. (a) Energy dependence of the density of states projected on the hydrogen atom on top at a distance $z = 2.4$ au from the graphene. In the inset we show the energy dependence of the corresponding $\mathrm{Re}[\Xi_{0\sigma}(\omega) + \Xi_{<\sigma}(\omega)]$ and their intersections with the $\omega - \varepsilon_{\mathrm{I}} - U$ straight lines. (b) Adiabatic charge state probability n_2 as a function of distance to the surface. The inset shows a blow up of the large distances region. The solid line corresponds to the calculation including all the effective interacting C atoms, the dashed–dotted line to the calculation including the first four neighbours and the dashed line to the calculation including only the C atom below.

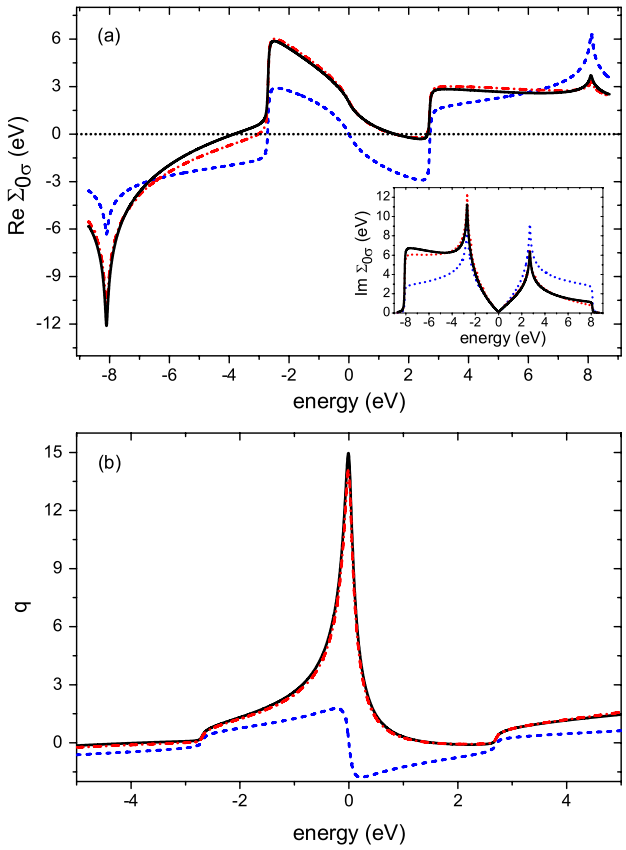

Figure 9. (a) Energy dependence of $\mathrm{Re}\,\Xi_{0\sigma}(\omega)$ for a hydrogen atom on top at a distance $z = 2.4$ au from the graphene. In the inset the corresponding $\mathrm{Im}\,\Xi_{0\sigma}(\omega)$ are shown. (b) The energy dependence of the q factor defined as $q = \mathrm{Re}\,\Xi_{0\sigma}(\omega)/\mathrm{Im}\,\Xi_{0\sigma}(\omega)$. The solid line corresponds to the calculation including all the effective interacting C atoms, the dashed–dotted line to the calculation including the first four neighbours and the dashed line to the calculation including only the C atom below.

electron loss when the affinity level is again above the Fermi level along the outgoing trajectory is drastically reduced due to the interference between neighbouring C atoms according to the results shown in figure 7. It is possible to explain in this form the large negative ion fraction measured in the case of hydrogen scattering by HOPG [20] at low normal to the surface velocity components. We can estimate roughly the charge state occupation of an atom colliding with a surface at low velocity within the semiclassical limit that neglects the quantum interferences inherent to a dynamical evolution. The objective in this case is to have only a qualitative idea of the incidence of the level broadening in a charge transfer process out of equilibrium. In this approximation the probability of charge exchange per unit of time is given by $2\Gamma_A(z)/\hbar$ and the following rate equation determines the time dependence of the hole state occupation when the spin fluctuation is also taken into account [37]:

$$\begin{aligned}\frac{\mathrm{d}\langle|\sigma\rangle\langle\sigma|\rangle}{\mathrm{d}t} &= 2\Gamma_A(z)[-\langle|\sigma\rangle\langle\sigma|\rangle(1 - f^{\mathrm{h}}_{<}(\varepsilon_a)) + \langle|0\rangle\langle 0|\rangle f^{\mathrm{h}}_{<}(\varepsilon_a)] \\ &= 2\Gamma_A(z)[-\langle|\sigma\rangle\langle\sigma|\rangle + [1 - \langle|\sigma\rangle\langle\sigma|\rangle]f^{\mathrm{h}}_{<}(\varepsilon_a)]. \qquad (18)\end{aligned}$$

In equation (18) $f^{\mathrm{h}}_{<}(\varepsilon_a) = 1 - f_{<}(\varepsilon_a)$ is the Fermi function for holes evaluated at the affinity energy. By considering the atom trajectory $z(t) = z_0 + v_{\mathrm{in(out)}}t$, with different velocities $v_{\mathrm{in(out)}}$ in the incoming and outgoing parts, we can write

$$\frac{\mathrm{d}\langle|\sigma\rangle\langle\sigma|\rangle}{\mathrm{d}z} = 2\frac{\Gamma_A(z)}{v_{\mathrm{in(out)}}}[-\langle|\sigma\rangle\langle\sigma|\rangle + [1 - \langle|\sigma\rangle\langle\sigma|\rangle]f^{\mathrm{h}}_{<}(\varepsilon_a)]. \qquad (19)$$

Figure 10 shows the evolution with distance of the double occupation n_2 in the case of an incoming kinetic energy $E_{\mathrm{k}} = 2$ keV and $v_{\mathrm{in(out)}}$ related to the perpendicular components of the velocity for trajectories with angles of $\theta_{\mathrm{in}} = 10°$ and $\theta_{\mathrm{out}} = 35°$ with respect to the surface plane (negative values of z represent the incoming trajectory). The movement perpendicular to the surface within an on top configuration is referred to the turning point z_0 chosen at 2 au from the surface. In this figure the results obtained by considering the interaction with one, four and the all involved C atoms are compared.

Charge and discharge processes take place depending on the atom level position and its width according to equation (19). The interaction with many C atoms determines an affinity level position which makes negative ion formation along the incoming part of the trajectory less favourable,

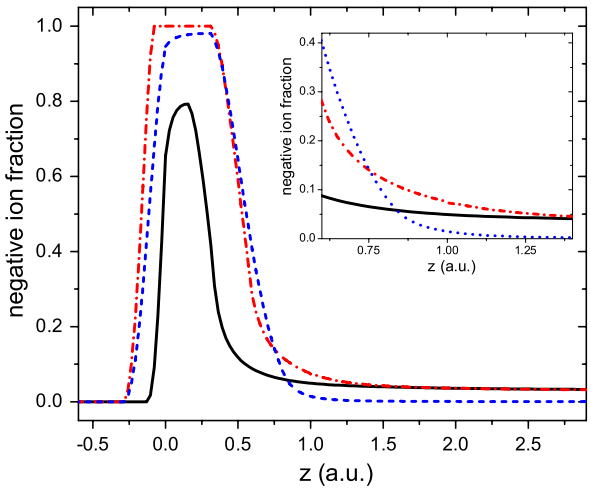

Figure 10. Double occupation probability n_2 as a function of distance to the surface obtained from the rate equation (equation (19)), by considering the interaction with only the C atom below (dashed line), the C below and its three first neighbours (dashed–dotted line) and all the C atoms that the hydrogen atom can see (solid line). The inset corresponds to a zoom of the exit trajectory at large distances.

but there is also less chance of electron loss during the exit trajectory due to the smaller level width (see figure 7). Finally, the diminished rate of electron loss in the case of considering properly the quantum-mechanical interference between the surface atoms involved in the interaction leads to a larger negative ion fraction. Notice that in the case of including only the first four C neighbours there is an increasing atom population to values near 1 close to the surface but a loss rate far from the surface considerably larger than in the case of considering all the C atoms able to interact with the hydrogen.

4. Conclusions

We have studied the interaction of a hydrogen atom with graphene by using an *ab initio* Anderson model. The effect of the quantum-mechanical interference between the neighbouring C atoms is analysed by varying the number of C atoms involved in the interaction. We find that the hybridization is strongly dependent on the adsorption site and that it is largely suppressed for the upper band energies. We also find a marked asymmetry of the hybridization function around the Fermi level due to the interference between the many C atoms able to interact with the hydrogen on top. This result leads to a relation $\mathrm{Re}\,\Xi_{0\sigma}(\omega)/\,\mathrm{Im}\,\Xi_{0\sigma}(\omega)$ strongly dependent on the energy and larger than 1 around the Fermi level, which suggests a Fano factor sensitive to local changes in the chemical potential of graphene. We treat the hydrogen neutral to negative charge fluctuation within an infinite intra atomic Coulomb repulsion approximation. The affinity level and its width validate the infinite U-limit approximation in the case of including the interaction with more than one C atom. The affinity level width is strongly reduced due to the quantum-mechanical interference associated with the graphene band structure. This result can explain the unexpectedly large negative ion fraction measured in the scattering of low energy protons by HOPG.

Acknowledgments

This work was supported by ANPCyT through PICT-07-0811 and UNL through CAI + D grants.

References

[1] Vergés J A and Andres P L 2010 *Phys. Rev.* B **81** 075423
[2] Bang J and Chang K J 2010 *Phys. Rev.* B **81** 193412
[3] Jacob D and Kotliar G 2010 *Phys. Rev.* B **82** 085423
[4] Boukhvalov D W, Katsnelson M I and Lichtenstein A I 2008 *Phys. Rev.* B **77** 035427
[5] Bostwick A, McChesney J L, Emtsev K V, Seyller T, Horn K, Kevan S D and Rotenberg E 2009 *Phys. Rev. Lett.* **103** 056404
[6] Yazyev O V and Helm L 2007 *Phys. Rev.* B **75** 125408
[7] Wehling T O, Dahal H P, Lichtenstein A I, Katsnelson M I, Manoharan H C and Balatsky A V 2010 *Phys. Rev.* B **81** 085413
[8] Khantha M, Cordero N A, Molina L M, Alonso J A and Girifalco L A 2004 *Phys. Rev.* B **70** 125422
[9] Novoselov K S, Geim A K, Morozov S V, Jiang D, Katsnelson M I, Grigorieva I V, Dubonos S V and Firsov A A 2005 *Nature* **438** 197
[10] Geimand A K S and Novoselov K 2007 *Nature Mater.* **6** 183
[11] Neto A H C, Guinea F, Peres N M R, Novoselov K S and Geim A K 2009 *Rev. Mod. Phys.* **81** 109
[12] Cornaglia P S, Usaj G and Balseiro C A 2009 *Phys. Rev. Lett.* **102** 046801
[13] Uchoa B, Kotov V N, Peres N M R and Neto A H C 2008 *Phys. Rev. Lett.* **101** 026805
[14] Uchoa B, Yang L, Tsai S W, Peres N M R and Neto A H C 2009 *Phys. Rev. Lett.* **103** 206804
[15] Anderson P W 1961 *Phys. Rev.* **124** 41
[16] Newns D M 1969 *Phys. Rev.* **178** 1123
[17] Muda Y and Newns D 1988 *Phys. Rev.* B **37** 7048
[18] Bonetto F, Romero M A, García E A, Vidal R A, Ferrón J and Goldberg E C 2008 *Phys. Rev.* B **78** 075422
[19] García E A, Romero M A, González C and Goldberg E C 2009 *Surf. Sci.* **603** 597
[20] Vidal R A, Bonetto F, Ferrón J, Romero M A, García E A and Goldberg E C 2011 *Surf. Sci.* **605** 18
[21] Nagaoka K, Jamneala T, Grobis M and Crommie M F 2002 *Phys. Rev. Lett.* **88** 077205
[22] Luo H G, Xiang T Q, Wang X, Su Z B and Yu L 2004 *Phys. Rev. Lett.* **92** 256602
[23] Néel N, Kröger J, Limot L, Palotas K, Hofer W A and Berndt R 2007 *Phys. Rev. Lett.* **98** 016801
[24] Merino J and Gunnarsson O 2004 *Phys. Rev. Lett.* **93** 156601
[25] Bolcatto P G, Goldberg E C and Passeggi M C G 1994 *Phys. Rev.* A **50** 4643
[26] Bolcatto P G, Goldberg E C and Passeggi M C G 1998 *Phys. Rev.* B **58** 5007
[27] Madhavan V, Chen W, Jamneala T, Crommie M F and Wingreen N S 2001 *Phys. Rev.* B **64** 165412
[28] Lowdin P O 1950 *J. Chem. Phys* **18** 365
[29] Keldysh L V 1964 *Zh. Eksp. Teor. Fiz.* **47** 1515
[30] Keldysh L V 1965 *Sov. Phys.—JETP* **20** 1018 (Engl. transl.)
[31] Romero M A and Goldberg E C 2006 *Phys. Rev.* B **74** 195419
[32] Huzinaga S 1965 *J. Chem. Phys.* **42** 1293
[33] Romero M A, Iglesias García A and Goldberg E C 2011 *Phys. Rev.* B **83** 125411
[34] Lehtinen P O, Foster A S, Ma Y, Krasheninnikov A V and Nieminen R M 2004 *Phys. Rev. Lett.* **93** 187202
[35] Duplock E J, Scheffler M and Lindan P J D 2004 *Phys. Rev. Lett.* **92** 225502
[36] Lewis J P, Glaesemann K R, Voth G A, Fritsch J, Demkok A, Ortega J and Sankey O F 2001 *Phys. Rev.* B **64** 195103
[37] Langreth D C and Nordlander P 1991 *Phys. Rev.* B **43** 2541